Steel and Composite Structures, *Vol. 15, No. 3 (2013) 343-355*
DOI: http://dx.doi.org/10.12989/scs.2013.15.3.343

Seismic responses of composite bridge piers with CFT columns embedded inside

Wenliang Qiu*[1], Meng Jiang [2a], Shengshan Pan [1b] and Zhe Zhang [1c]

[1] *School of civil engineering, Dalian University of Technology, Dalian, P.R. China*
[2] *School of hydraulic engineering, Dalian University of Technology, Dalian, P.R. China*

(Received January 10, 2012, Revised April 26, 2013, Accepted July 19, 2013)

Abstract. Shear failure and core concrete crushing at plastic hinge region are the two main failure modes of bridge piers, which can make repair impossible and cause the collapse of bridge. To avoid the two types of failure of pier, a composite pier was proposed, which was formed by embedding high strength concrete filled steel tubular (CFT) column in reinforced concrete (RC) pier. Through cyclic loading tests, the seismic performances of the composite pier were studied. The experimental results show that the CFT column embedded in composite pier can increase the flexural strength, displacement ductility and energy dissipation capacity, and decrease the residual displacement after undergoing large deformation. The analytical analysis is performed to simulate the hysteretic behavior of the composite pier subjected to cyclic loading, and the numerical results agree well with the experimental results. Using the analytical model and time-history analysis method, seismic responses of a continuous girder bridge using composite piers is investigated, and the results show that the bridge using composite piers can resist much stronger earthquake than the bridge using RC piers.

Keywords: reinforced concrete; concrete filled steel tube; composite pier; seismic responses; cyclic loading tests; damage; ductility

1. Introduction

The past strong earthquakes in the world show that the reinforced concrete (RC) piers of girder bridges have two main failure modes, which lead to severe damages of piers, such as collapse and being un-repairable (Chen and Duan 1999, Hsu and Fu 2004, Hashimoto *et al*. 2005). One mode is the shear failure because of insufficient shear capacity of pier, and the other is core concrete crushing at plastic hinge region because of insufficient ductility of pier. So the shear capacity and ductility are critically important seismic performance of bridge piers. To enhance the shear capacity and ductility of RC bridge piers, the generally used method is to increase the lateral reinforcements (Chen and Duan 1999). Excessive use of reinforcements, however, can become counterproductive in terms of both constructability and economy (Pandey and Mutsuyoshi 2005).

*Corresponding author, Professor, E-mail: qwl@dlut.edu.cn
[a] Associate Professor, E-mail: jiangm@dlut.edu.cn
[b] Associate Professor, E-mail: pssbu@dlut.edu.cn
[c] Professor, E-mail: zhangzhe@dlut.edu.cn

http://www.techno-press.org/?journal=scs&subpage=8 ISSN: 1229-9367 (Print), 1598-6233 (Online)

It is therefore important to find alternative methods of improving shear capacity and ductility to avoid relying heavily on lateral reinforcements alone.

Concrete filled steel tube (CFT) is a kind of composite structure, which has many advantages, such as high flexural, compressive and shear capacity and high ductility (Roeder and Lehman 2009, Zhang *et al*. 2010). But when used as bridge pier, CFT has many disadvantages. Because the flexural capacity of CFT pier is high, the connection between CFT pier and foundation is complicated and difficult (Roeder and Lehman 2009). Additionally, the steel tube needs to be protected from rust.

In this paper, the CFT column is put into the RC pier to form a new kind of composite pier. This kind of composite pier can take advantages of both CFT and RC piers, and avoid their disadvantages. The composite pier use CFT column to improve the shear capacity and ductility of RC pier, and avoid core concrete crushing at plastic hinge region. To make construction of the concrete outside of steel tube and connection with the foundation easy and feasible, the diameter of the CFT column in composite pier cannot be too large, although larger value is beneficial for improving the seismic performances of the composite pier. So the value of about 1/3 of the RC pier diameter is recommended. To improve the ductility of composite pier, the concrete outside the steel tube adopts normal strength concrete, which is more ductile than high strength concrete (Cusson and Paultre 1994, Sun *et al*. 2010). The concrete in steel tube adopts high strength concrete to increase the compressive capacity of the CFT column.

To be able to apply this kind of composite bridge pier presented here in actual construction, seismic performances such as shear strength, flexural strength, ductility, residual displacement and energy absorption capacity must be investigated. Therefore, the seismic performances of the composite pier are investigated in this paper.

2. Experimental programs

2.1 Specimens

To investigate the seismic performances of the composite pier with CFT column embedded inside, two bridge pier specimens with circular section were designed in this study, as shown in Fig. 1. The alphanumeric designations of the two specimens were CR302 and CS302. The pier CR302 was a conventional reinforced concrete pier, which served as the comparative specimen with pier CS302. The pier CS302 was a composite piers with a CFT column inside. The diameter of each pier was 300 mm, the height of pier was 1000 mm. The action point of cyclic lateral load was at the height of 900 mm from the footing. So the aspect ratio (the pier height from the footing to the lateral load action point divided by the pier diameter) was 3.0. The footing of the pier was designed strong enough to avoid damage and reduce the deformation of footing. The footing was anchored to the strong floor by steel rods. The axial load index (ALI) of the each two pier was designed to be about 0.2. The ALI was defined as the ratio of the axial load to the product of the specified compressive strength of concrete and the gross pier cross section area.

2.2 Reinforcement, concrete and steel tube

Each pier was reinforced with eight longitudinal reinforcement bars evenly spaced in circular pattern. The diameter of longitudinal reinforcement was 14 mm. The reinforcement ratio was 1.74%.

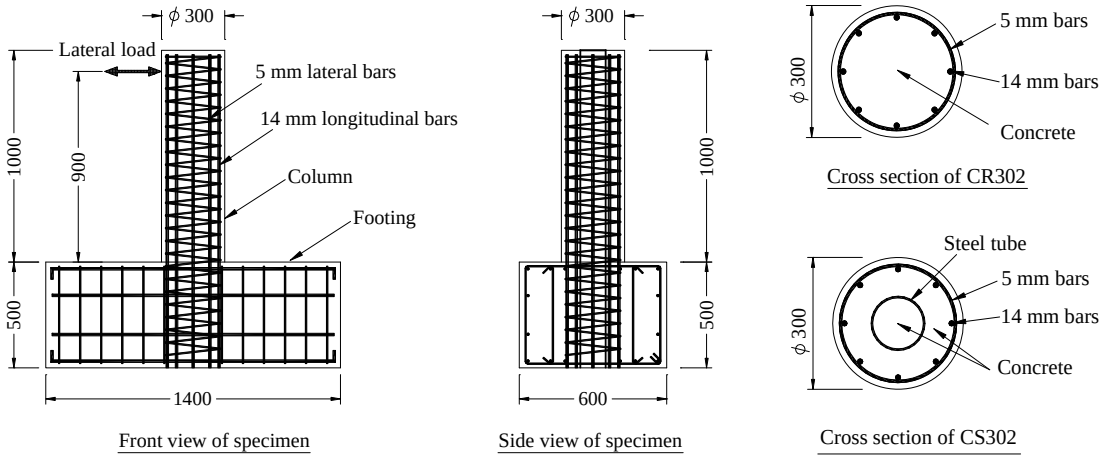

Fig. 1 Reinforcing details of specimens (dimensions in mm)

The lateral spiral reinforcement was a round bar with a diameter of 6 mm and a pitch of 50 mm. The clear concrete cover of lateral reinforcement was 25 mm. The yield stress of longitudinal reinforcement was 345 MPa, and the yield stress of lateral reinforcement was 235 MPa.

The concrete of pier CR302 and the concrete outside of pier CS302 was normal strength concrete with compressive strength of 32.4 MPa at 28 days. The concrete in steel tube was high strength concrete with compressive strength of 54.3 MPa at 28 days. All of the concrete was constructed on the same day.

The diameter of steel tube in pier CS302 was 121 mm, and the wall thickness of the tube was 5.3 mm. The yield stress of steel tube was 345 MPa. The length of CFT column embedded in footing was 450 mm.

2.3 Test setup and loading method

The seismic performance experiments of the specimens were accomplished in a structural testing laboratory with a hydraulic jack and an actuator. Fig. 2 shows the experimental setup employed in this study. The axial load applied at the beginning of a test and maintained constant during testing was applied by a vertical hydraulic jack, which moved with the tip of pier. The cyclic lateral load was applied by the horizontal actuator. Two ends of the actuator were bolted to the reaction wall and the pier head. The actuator had a capacity of 1000 kN and was capable of moving the pier 150 mm in both pull and push direction. The vertical axial load was used to simulate the weight of girder, and the cyclic lateral load was used to simulate the seismic load. The load cells were used to measure and control the forces of the hydraulic jack and the actuator. Foil strain gauges on surfaces of reinforcements and steel tube and displacement transducers at the top of pier and the footing were used to record the responses of the pier. According to the designed ALI of about 0.2, the axial loads applied on specimens were 300 kN.

The lateral load was applied at a quasi-static rate in displacement-controlled cycles to ± 2 mm, ± 4 mm, ± 6 mm, ± 8 mm, ± 12 mm, ± 18 mm, ± 24 mm, ± 36 mm, ± 48 mm, ± 60 mm, ± 72 mm, ± 84 mm, ± 96 mm, etc. The lateral displacement history is shown in Fig. 3. Three cycles were run

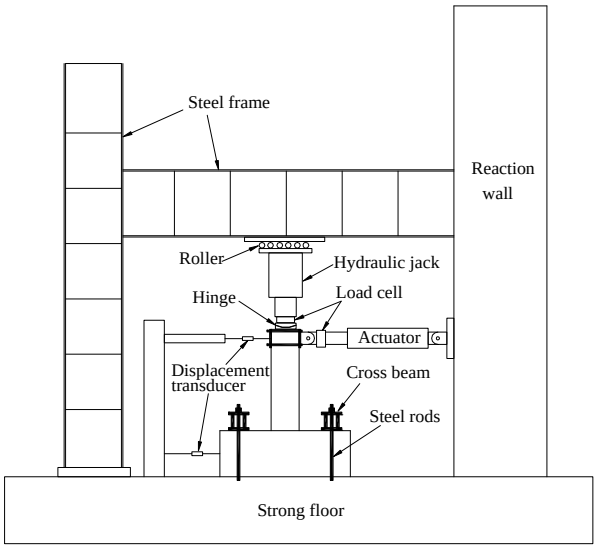

Fig. 2 Experimental setup

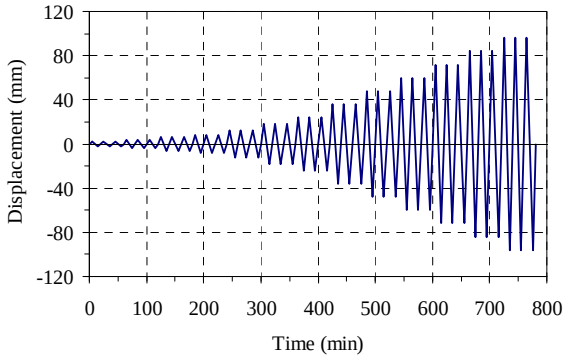

Fig. 3 Displacement history

at each displacement amplitude. When the core concrete of pier crushed or the lateral load capacity of pier decreased to 80% of its maximum lateral load, the test was terminated.

3. Experimental results

3.1 Apparent damage

3.1.1 Pier CR302

For CR302, when the top pier lateral displacement amplitude reached 2 mm, there were no cracks occurring on the pier, and the maximum lateral load in three cycles was 44.7 kN. When the lateral displacement amplitude reached 4 mm, several horizontal cracks occurred on each side of the pier from the footing to the half height of the pier. The widths of cracks were very small, and the cracks were closed under a zero lateral load in the actuator. The maximum lateral load in three cycles was 60.8 kN. In subsequent displacement amplitudes, the number of horizontal cracks increased little, but the widths of crack increased markedly. When the lateral displacement amplitude reached 18 mm, initial spalling of the cover concrete occurred near the footing. At the same time, several vertical cracks occurred. The maximum lateral load in three cycles was 85.3 kN. When the lateral displacement amplitude reached 24 mm, some blocks of cover concrete on both sides of the pier in the loading direction spalled off. When the lateral displacement amplitude reached 36 mm, the spiral and longitudinal reinforcement on both sides of the pier in the loading direction were exposed entirely because the cover concrete spalled off. The height of spalling region was about 160 mm from the pier footing. The maximum lateral load dropped to 82.7 kN, which is smaller than the maximum load occurring previously. When the lateral displacement amplitude reached 48 mm, the spiral reinforcement extruded, and the longitudinal reinforcement buckled. At the same time, a diagonal shear crack occurred from footing to the height of 190 mm, as shown in Fig. 4. When the lateral displacement amplitude reached 60 mm, the spiral

(a) CR302

(b) CS302

Fig. 4 Damage of specimens

reinforcement yielded, the longitudinal reinforcement buckled seriously, and the lateral load capacity dropped to 57.5 kN. The loading test was terminated after the specimen underwent three cycles at displacement amplitude of 72 mm because the lateral load capacity dropped to 34.6 kN.

3.1.2 Pier CS302

When the lateral displacement amplitude was less than 48 mm, the cracking and cover concrete spalling of pier CS302 were similar with those of pier CR302. But the maximum lateral load was 127.8 kN, which was much larger than the maximum lateral load of pier CR302 by 51.3%. The spalling height of the cover concrete from the footing is 140 mm, which was less than that of pier CR302. No diagonal shear crack occurred in pier CS302 during the whole loading test, which showed that the CFT column embedded in RC pier could prevent the pier from shear failure, as shown in Fig. 4. When the lateral displacement amplitude reached 60 mm, the spiral reinforcement yielding and the longitudinal reinforcement buckling were not observed obviously. It showed that the CFT column in composite pier could help the RC pier to share very significant part of the axial load, which could postpone the buckling of longitudinal reinforcement. When the lateral displacement amplitude reached 72 mm, the longitudinal reinforcement began to buckle after three cycles. The lateral load capacity dropped to 88.4 kN that was smaller than 80% of the maximum lateral load occurring previously, and the test was terminated.

3.2 Load-displacement relationship

Fig. 5 shows the lateral load-displacement hysteretic curves of the two piers that were subjected to the reversed cycling load. The lateral displacement of the pier is the displacement at the point where the lateral load was applied. It is found that the hysteretic curves of the piers are very wide. The two piers have ductile and stable behaviors under cyclic loads. For pier CR302, the curves of three loading cycles at the same displacement amplitude are overlapped when the displacement amplitude is small. But they are separated from each other with the displacement amplitude increasing. When the displacement amplitude is large, every loading cycle leads to obvious damage accumulation in pier CR302, and the lateral load capacity of pier CR302 decreases after each loading cycle. The two piers show obvious damage accumulation and reduction of load capacity at the displacement amplitude of 20-40 mm, but load capacity of composite pier decreases

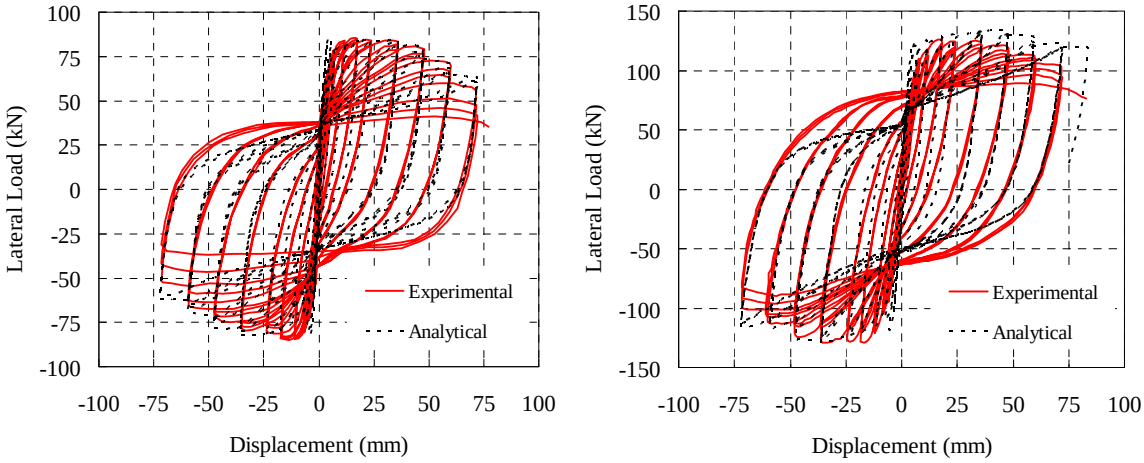

(a) CR302 (b) CS302

Fig. 5 Load-displacement hysteretic curves

more slowly than RC pier after the displacement amplitude is larger than 40 mm. So the CFT column in composite pier can reduce the damage degree of the pier and make the pier more stable under cyclic loads.

Lateral load capacities of piers CR302 and CS302 are respectively 85.3 kN and 127.8 kN. The lateral load capacity of pier CS302 is larger than that of pier CR302 by 49.8%. So the CFT column in composite pier can markedly enhance the lateral load capacity of pier.

To compare the stiffness and ductility of the two piers, the envelopes of measured load-displacement relationships are depicted in one figure, as shown in Fig. 6. At forehead loading stage, the stiffness of pier CS302 are nearly same as that of pier CR302 when the displacement is small, which shows that the CFT column with small diameter has little influence on initial flexural

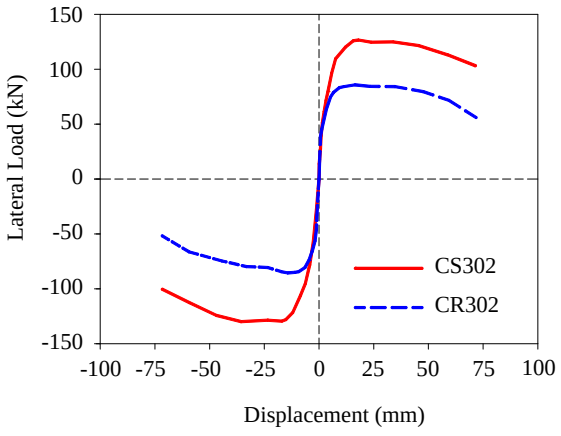

Fig. 6 Envelopes of load-displacement hysteretic curves

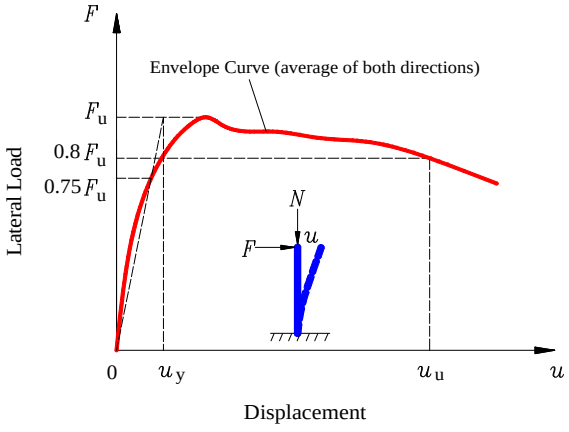

Fig. 7 Ideal curve definitions

Table 1 Ductility of piers

Specimen	Maximum force F_u (kN)	Yielding displacement u_y (mm)	Ultimate displacement u_u (mm)	Ultimate drift ratio u_u / L (%)	Ductility factor u_u / u_y
CR302	85.3	4.2	59.9	6.7	14.3
CS302	127.8	8.1	71.2	7.9	8.8

stiffness of composite pier. But the stiffness of pier CS302 is larger than that of pier CR302 when the displacement is large.

3.3 Ductility

Ductility factor is usually used to evaluate the seismic response of reinforced concrete members (Légeron and Paultre 2000, Paultre *et al*. 2001). The displacement ductility factor is defined as the ultimate displacement divided by the yield displacement. The ultimate displacement is defined as the displacement at 80% of the maximum lateral load in the descending portion of the lateral load-displacement relationship. The yield displacement is defined as the displacement obtained from the intersection point of the horizontal line at the maximum lateral load and the straight line from the origin passing through the point on the load-displacement plot at 75% of the maximum lateral load (Zahn *et al*. 1990). The definition of the maximum lateral load F_u, the ultimate displacement u_u and the yield displacement u_y are shown in Fig. 7. The load-displacement relationship curve is the average of the envelope for the push-and-pull loading.

Ultimate displacements, yield displacements, displacement ductility factors and ultimate drift ratios (defined as the ultimate displacement divided by height of lateral loading point from pier footing) of the two piers are listed in Table 1. The ultimate displacement of piers CR302 and CS302 are respectively 59.9 mm and 71.2 mm. The ultimate displacement of pier CS302 is larger than that of pier CR302 by 18.9%. The displacement ductility factor of pier CR302 is the larger than CS302, but the ultimate drift ratio of pier CS302 is larger than CR302.

3.4 Residual displacement

Residual displacement is a very important factor to determine if the bridge undergoing strong earthquake is removed or not. Large residual inclination of pier makes the placement of the girders difficult and causes visual uneasiness even if repair is possible. After Kobe earthquake, the piers with residual inclination larger than 1º were removed even if their visually judged damage was mild (Fujino *et al*. 2005, Fahmy *et al*. 2009). So reducing the residual displacement of pier is a very important aspect in improving the seismic performance of bridge pier. Fig. 8 presents the relationships of the residual displacements of the two tested piers and the maximum displacement reached. When the displacement amplitude is less than 8 mm, the residual displacements of the two piers are less than 17% of the corresponding displacement amplitude. When the displacement amplitudes are larger than 12 mm, the ratios of residual displacements to the corresponding displacement amplitudes increase rapidly with the displacement amplitude increasing. For pier CS302, the ratios are 0.48, 0.70, 0.78 and 0.84, when the displacement amplitudes are respectively 20 mm, 40 mm, 60 mm and 72 mm. For pier CR302, the ratios are correspondingly 0.42, 0.69,

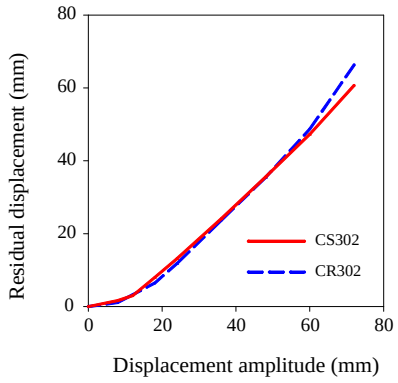

Fig. 8 Residual displacement comparison

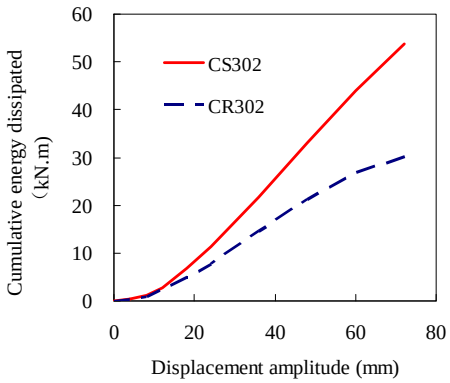

Fig. 9 Cumulative energy dissipation of specimens

0.81 and 0.92. When the displacement amplitude is smaller than 60 mm, the two curves are nearly overlapped. When the displacement amplitude is larger than the ultimate displacement of pier CR302, the residual displacement of pier CR302 increases more rapidly than that of pier CS302. So the composite pier can reduce the residual displacement when it undergoes strong earthquake.

3.5 Energy dissipation

The energy dissipation capacity is critically important for the seismic performance of bridge pier (Légeron and Paultre 2000, Paultre *et al*. 2001). The dissipated energy can be determined by integrating the areas bounded by all the hysteretic loops of the whole loading test (Paultre *et al*. 2009). Fig. 9 presents the cumulative energy dissipation-displacement amplitude relationships of the piers CR302 and CS302. When the displacement is small, the energy dissipation curves of the two piers are not obviously different from each other. But with the displacement increasing, the difference becomes larger and larger. It is concluded that the CFT column in composite pier can markedly improve the energy dissipation capacity of bridge pier, which is very benefit for the bridge to resist strong earthquake.

4. Numerical studies of bridge pier

4.1 Analytical model of bridge pier

The analytical modeling of bridge pier performed herein is done using the OpenSees platform, (opensees.berkeley.edu). The piers are modeled with nonlinear beam-column elements. The nonlinear beam-column element used here is a fiber-based element with nonlinear constitutive behavior, as shown in Fig. 10. In the fiber model, the element is divided into some fibers along the longitudinal direction, if the number of the fibers is large enough, every fiber can be treated as only having axial strain, and its curvature can be neglected. The strain of every fiber is calculated by the axial strain and curvature of section. So the moment-curvature relationship of every section can be determined by the stress-strain relationship of the materials and strain distribution on the section.

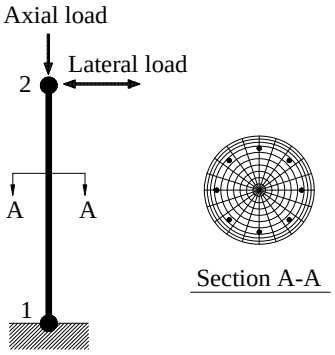

Fig. 10 Fiber element model of pier

4.2 Constitutive relationship of materials

When the nonlinear analysis of RC pier and composite pier are performed, the constitutive relationships of concrete, reinforcement and steel tube are needed.

The concrete inside of transversal reinforcement and steel tube adopts the constitutive relationship of confined concrete, and the concrete outside of transversal reinforcement adopts the constitutive relationship of unconfined concrete. The cyclic behaviors of unconfined and confined concrete are modeled by Concrete07, which generally follow the hysteretic rules proposed by Chang and Mander (1994). These rules were established based on statistical regression analysis on the experimental data from cyclic compression tests of a number of researchers. For the reason of computational efficiency and numerical stability, some of the rules are simplified in Concrete07. The tension strength of concrete is neglected in the cyclically loading analysis, because the concrete cracks at the small displacement and can not bear tension after cracking.

The unconfined compressive strength of the concrete taken as cylindrical compression strength can be measured, and the strain at peak stress is usually taken as 0.002. For the core concrete confined by spiral reinforcing, the peak compressive stress and strain are increased due to the confinement effect based on the Mander *et al*. (1983) model. For the core concrete confined by circular steel tube, the peak compressive stress and strain are increased due to the confinement effect based on the Sakino *et al*. (1998) model.

The stress-strain relationship for the bonded longitudinal reinforcing steel and steel tube is described by the Giuffre-Menegotto-Pinto model (Taucer *et al*. 1991), which incorporates the Bauschinger effect for cyclic loading. For simplicity, bond slip in the reinforcing is not included in the model. Steel yield strengths are based on tensile tests of the reinforcing bars and steel tube. A hardening ratio of 1% is assumed.

4.3 Analytical results

Using the above mentioned finite element model and constitutive relationship of materials, The relationship of lateral load and top displacement of piers CR302 and CS302 subjected to cyclic load are simulated. The analytical results are shown in Fig. 5. From the comparison, it is found that the numerical results agree with the experimental results very well. So the analytical model can be used to simulate nonlinear behavior of the composite pier. The analytical model is used to

analyze the seismic responses of bridge adopting composite piers in the following section.

5. Seismic responses of bridge adopting composite piers

5.1 Introduction of the studied bridge

Taking a 3-span continuous girder bridge built in China shown in Fig. 11 with a span length of 30 m as a numerical example, the seismic responses of two continuous girder bridges, one adopting composite piers and the other adopting RC piers, are studied. The main girder is prestressed concrete box girder. The weight of each span girder is 12460 kN. In original design, circular section RC piers with diameter of 1.5 m are adopted as piers. The cylinder compressive strength of concrete is 30 MPa, the tensile strength is ignored, and the initial Young's modulus is 2.76e4 MPa. In one RC pier, 30 steel bars with a diameter of 32 mm are used as longitudinal bars, and circular steel stirrups with a diameter of 16 mm and with pitch of 100 mm are adopted. The yield strength of the steel bar is 335 MPa, and the initial Young's modulus is 2.06e5 MPa. The composite pier is formed by embedding a CFT column with a diameter of 500 mm into the previous RC pier. The wall thickness of steel tube is 16 mm, and the cylinder compressive strength of concrete in steel tube is 50 MPa.

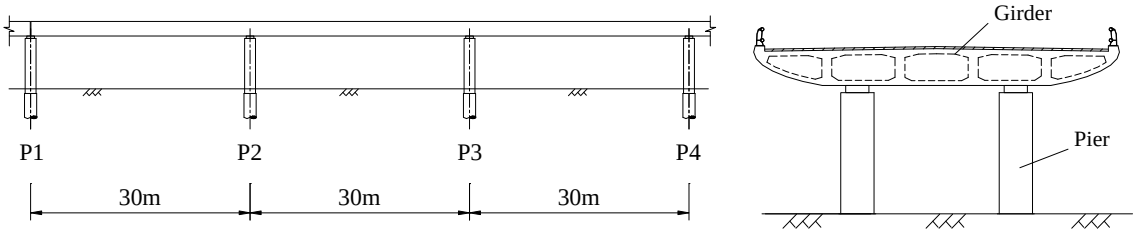

(a) Elevation (b) Section

Fig. 11 The continuous girder bridge

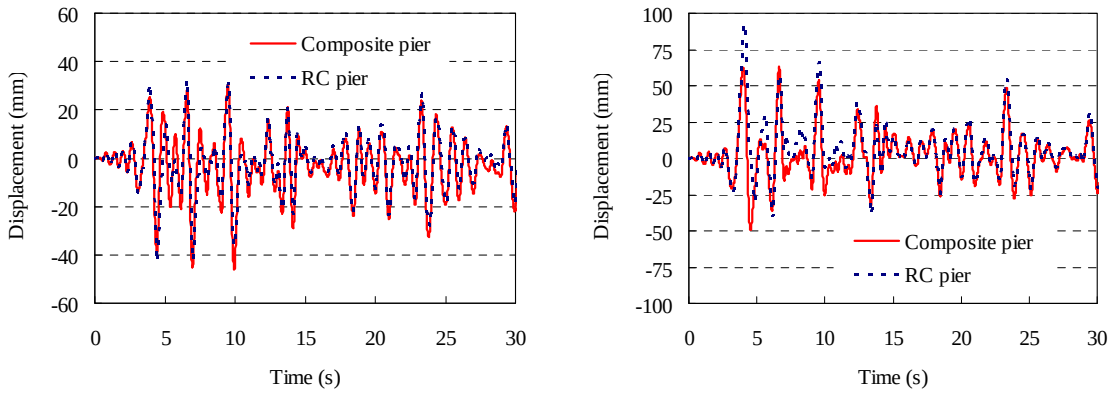

(a) 0.2 g (b) 0.3 g

Fig. 12 Displacement histories of pier P2

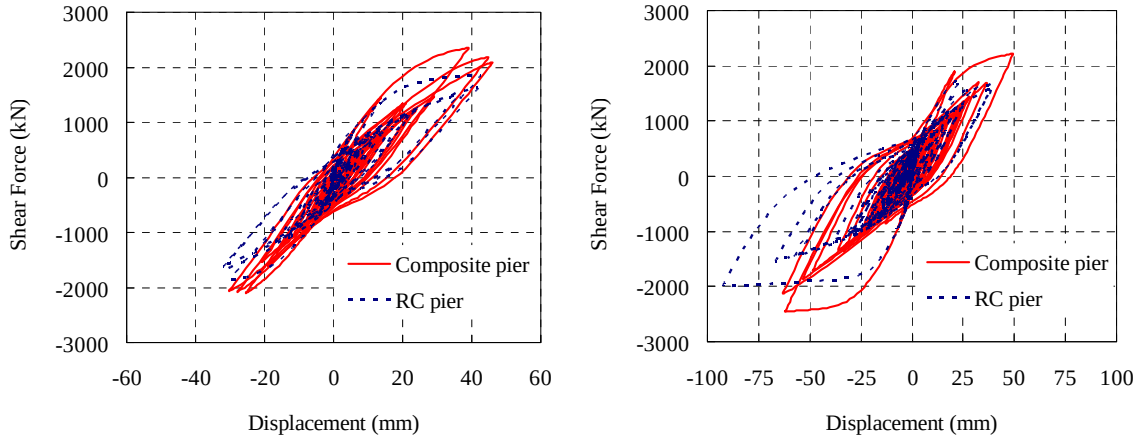

(a) 0.2 g (b) 0.3 g

Fig. 13 Shear force-displacement hysteretic curves of pier P2

Taft seismic wave (1952, Taft Lincoln School) is adopted in the nonlinear time-history analysis. The peak earthquake acceleration is adjusted to be the value needed. The wave is input longitudinally. In order to make the study results representative, the heights of all piers take the value of 5 m. The OpenSees platform is used to analyze the seismic performance of the bridge. Because pier P2 adopts fixed bearing and the other piers adopt expansion bearings in the bridge, the seismic response analysis mainly focuses on pier P2. The damping ratio of the structure is taken as 2% in the analysis.

5.2 Seismic responses

The displacement histories and the hysteretic curves of shear force-displacement of the top of pier P2 under different intensity earthquake are shown in Figs. 12 and 13. When the peak acceleration of the seismic wave is 0.2 g, there is nearly no difference between the displacement histories of composite pier and RC pier, but the maximum shear force of composite pier is larger than that of RC pier.

When the peak acceleration of the seismic wave is 0.3 g, the difference between the displacement histories of composite pier and RC pier is very obvious. The maximum displacement of composite pier is 62.0 mm, and the maximum displacement of RC pier is 91.6 mm. The maximum shear force of composite pier is 2453.2 kN, and the maximum shear force of RC pier is 1930.8 kN. So the composite pier can reduce the displacement and increase the energy dissipating capacity by its large flexural strength. From the previous experimental studies, it is known that the ultimate displacement of composite pier is much larger than RC pier. So it can be concluded that the bridge using composite piers can resist much stronger earthquake than bridge using RC piers.

6. Conclusions

Based on the experimental and numerical results in this paper, the following key conclusions can be reached:

(1) The CFT column in composite pier can enhance the flexural strength, shear strength and energy dissipation capacity of the pier, and avoid the shear failure and core concrete crushing of the pier effectively. The lateral load capacity of composite pier is larger and more stable than that of RC pier. The energy dissipation capacity of composite pier is much larger than that of RC pier, especially when the displacement is large. This is very beneficial for the bridge to resist strong earthquake.
(2) Before the lateral tip displacement of pier reaches its ultimate displacement, the CFT pier has little effects on the residual displacement of composite pier. After the lateral displacement of pier exceeds its ultimate displacement, the residual displacement of RC pier increases very quickly, but the residual displacement of composite pier increases stably with the lateral displacement of pier increasing.
(3) Fiber element model and existed constitutive relationships of material can be used to simulate the nonlinear behavior of composite pier subjected to cyclic loading. The numerical results agree well with the experimental results. The continuous girder bridge using composite piers can resist much stronger earthquake than the bridge using RC piers.
(4) For composite pier with diameter of 300 mm, CFT column with diameter of about 1/3 of the composite pier diameter does not affect the concrete construction quality, and the CFT column is easy to be connected with the footing.

Acknowledgements

This study is funded by the National Natural Science Foundation of China (NSFC-51178080). The author would like to acknowledge the Structure Engineering Laboratory of Dalian University of Technology for the support and constructive advices.

References

Chang, G.A. and Mander, J.B. (1994), "Seismic energy based fatigue damage analysis of bridge columns", *Technical Report NCEER-94-0006*, University at Buffalo, State University of New York.

Chen, W.F. and Duan, L. (1999), *Bridge Engineering Handbook*, CRC press LLC.

Cusson, D. and Paultre, P. (1994), "High-strength concrete piers confined by rectangular ties", *J. Struct. Eng., ASCE*, **120**(3), 783-804.

Fahmy, M.F.M., Wu, Z.S. and Wu, G. (2009), "Seismic performance assessment of damage-controlled FRP-retrofitted RC bridge columns using residual deformations", *J. Compos. Constr.*, **13**(6), 498-513.

Fujino, Y., Hashimoto, S. and Abe, M. (2005), "Damage analysis of Hanshin expressway viaducts during 1995 Kobe Earthquake. I: residual inclination of reinforced concrete piers", *J. Bridge Eng.*, **10**(1), 45-53.

Hashimoto, S., Fujino, Y. and Abe, M. (2005), "Damage analysis of Hanshin expressway viaducts during 1995 Kobe Earthquake. II: damage mode of single reinforced concrete Piers", *J. Bridge Eng.*, **10**(1), 54-60.

Hsu, Y.T. and Fu, C.C. (2004), "Seismic effect on highway bridges in Chi Chi Earthquake", *J. Perform. Constructed Facil.*, **18**(1), 869-879.

Légeron, F. and Paultre, P. (2000), "Behavior of high-strength concrete piers under cyclic flexure and constant axial load", *ACI Struct. J.*, **97**(4), 591-601.

Mander, J., Priestley, M.N. and Park, R. (1983), "Seismic design of bridge piers", Rep. No. 84-02, University of Canterbury, Christchurch, New Zealand.

Pandey, G.R. and Mutsuyoshi, H. (2005), "Seismic performance of reinforced concrete piers with

bond-controlled reinforcements", *ACI Struct. J.*, **102**(2), 295-304.
Paultre, P., Eid, R., Robles, H.I. and Bouaanani, N. (2009), "Seismic performance of circular high-strength concrete piers", *ACI Struct. J.*, **106**(4), 395-404.
Paultre, P., Légeron, F. and Mongeau, D. (2001), "Influence of concrete strength and yield strength of ties on the behavior of high-strength concrete piers", *ACI Struct. J.*, **98**(4), 490-501.
Roeder, C.W. and Lehman, D.E. (2009), "Research on rapidly constructed CFT bridge piers suitable for seismic design", *Lifeline Earthquake Engineering in a Multihazard Environment ASCE* (*TCLEE 2009*), 24-34.
Sakino, K., Ninakawa, T., Nakahara, H. and Morino, S. (1998), "Experimental studies and design recommendations on concrete filled steel tubular columns—U.S.-Japan Cooperative Earthquake Research Program", S*tructural Engineers World Congress*, N.K. Srivastava, July.
Sun, Z.G., Si, B.J., Wang, D.S., Guo, X. and Yu, D.H. (2010), "Research on the seismic performance of high-strength concrete column with high-strength stirrups", *Engineering Mechanics*, **27**(5), 128-136. (In Chinese)
Taucer, F., Spacone, E. and Filippou, F. (1991), "A fiber beam-column element for seismic response analysis of reinforced concrete structures", UCB/EERC Technical Rep. No. 91/17, Earthquake Engineering Research Center, University of California, Berkeley, CA.
Zahn, F.A., Park, R. and Priestley, M.J.N. (1990), "Flexural strength and ductility of circular hollow reinforced concrete piers without confinement on inside face", *ACI Struct. J.*, **87**(2), 156–166.
Zhang, H., Liu, Z. and Li, H.Y. (2010), "Experimental study on seismic performance of concrete-filled steel bridge piers", *J. Disaster Prevention Mitigation Eng.*, **30**(4), 442-446. (In Chinese)

CC